Improving Arctic sea ice seasonal outlook by ensemble prediction using an ice-ocean model

Qinghua Yang[1,2,3], Longjiang Mu[4]*, Xingren Wu[5], Jiping Liu[6], Fei Zheng[7], Jinlun Zhang[8], Chuanjin Li[2]

1. Guangdong Province Key Laboratory for Climate Change and Natural Disaster Studies, and School of Atmospheric Sciences, Sun Yat-sen University, Zhuhai, China
2. State Key Laboratory of Cryospheric Science, Northwest Institute of Eco-Environment and Resources, Chinese Academy Sciences, Lanzhou, China
3. Southern Marine Science and Engineering Guangdong Laboratory (Zhuhai), Zhuhai, China
4. Alfred Wegener Institute, Helmholtz Centre for Polar and Marine Research, Bremerhaven, Germany
5. National Center for Environmental Prediction (NCEP), Maryland, US
6. Department of Atmospheric and Environmental Sciences, University at Albany, State University of New York, Albany, New York, US
7. International Center for Climate and Environment Sciences, Institute of Atmospheric Physics, Chinese Academy of Sciences, Beijing, China
8. Polar Science Center, Applied Physics Laboratory, University of Washington, Seattle, Washington, US

Correspondence to: L. Mu (longjiang.mu@awi.de)

Abstract

An ensemble based Sea Ice Seasonal Prediction System (SISPS) is configured towards operationally predicting the Arctic summer sea ice conditions. SISPS runs as a pan-Arctic sea ice-ocean coupled model based on Massachusetts Institute of Technology general circulation model (MITgcm). A 4-month hindcast is carried out by SISPS starting from May 25, 2016. The sea ice-ocean initial fields for each ensemble member are from corresponding restart files from an ensemble data assimilation system that assimilates near-real-time Special Sensor Microwave Imager Sounder (SSMIS) sea ice concentration, Soil Moisture and Ocean Salinity (SMOS) and CryoSat-2 ice thickness. An ensemble of 11 time lagged operational atmospheric forcing from the National Center for Environmental Prediction (NCEP) climate forecast system model version 2 (CFSv2) is used to drive the ice-ocean model. Comparing with the satellite based sea ice observations and reanalysis data, the SISPS prediction shows good agreement in the evolution of sea ice extent and thickness, and performs much better than the CFSv2 operational sea ice prediction. This can be largely attributed to the initial conditions that we used in assimilating the SMOS and CryoSat-2 sea ice thickness data, thereafter reduces the initial model bias in the basin wide sea ice thickness, while in CFSv2 there is no sea ice thickness assimilation. Furthermore, comparisons with sea ice predictions driven by deterministic forcings demonstrate the importance of employing an ensemble approach to capture the large prediction uncertainty in Arctic summer. The sensitivity experiments also show that the sea ice thickness initialization that has a long-term memory plays a more important role than sea ice concentration and sea ice extent initialization on seasonal sea ice prediction. This study shows a good potential to implement Arctic sea ice seasonal prediction using the current configuration of ensemble system.

Keywords: seasonal sea ice prediction, ensemble forecast, sea ice thickness, data assimilation

1. Introduction

Arctic sea ice is under dramatic shrinking and thinning (e.g., Cavalieri and Parkinson, 2012; Kwok and Cunningham, 2015). The opening of commercial shipping routes in the Arctic Ocean significantly reduces the shipping distance from Asia to Europe. The reliable sea ice prediction from daily to seasonal scale is thus strongly required by the increasing shipping activities in the Arctic (Jung et al., 2016). Not only is the real-time prediction on the synoptic scale strongly needed during shipping in the Arctic, the seasonal sea ice outlook is also required for better decisions on the shipping time window before the coming summer.

Since 2008, the international communities have made great efforts to predict the Arctic summer sea ice minimum from late May or early June (Sea Ice Outlook (SIO), http://www.arcus.org/sipn/sea-ice-outlook;

Stroeve et al., 2014). The employed approaches include statistical models, sea ice-ocean models (e.g., Pan-Arctic Ice Ocean Modeling and Assimilation System (PIOMAS), Zhang et al., 2008) and fully coupled atmosphere-sea ice-ocean models (e.g., the National Centers for Environmental Prediction (NCEP) climate forecast system version 2 (CFSv2), Saha et al., 2014). Fully coupled models allow a strong interaction between the atmosphere, sea ice and ocean and are more complex (Kauker et al., 2015), while sea ice-ocean models are forced by prescribed atmospheric fields and are easier to implement. Nevertheless, the 10-year international joint efforts using these approaches from Sea Ice Prediction Network (SIPN) show that the seasonal Arctic sea ice prediction remains challenging with large uncertainties.

Numerical predictions depend heavily on the initial sea ice model states. Systematic use of sea ice observations in an advanced data assimilation system is crucial for the sea ice prediction (Yang et al., 2014, 2015). The sea ice thickness initialization has been shown to be important for seasonal Arctic sea ice prediction (e.g., Blanchard-Wrigglesworth et al., 2011; Chevallier and Salas-Melia, 2012; Day et al., 2014; Massonnet et al., 2014). In recent years, basin-scale sea ice thickness data from satellites have become available, e.g., the Soil Moisture and Ocean Salinity (SMOS) sea ice thickness (Tian-Kunze et al., 2014) and the CryoSat-2 sea ice thickness (Ricker et al., 2014). However, very limited studies examined the potential influence of assimilating SMOS and/or CryoSat-2 ice thickness on the seasonal sea ice prediction to date (e.g., Kauker et al., 2015; Chen et al., 2017; Blockley et al., 2018).

Based on ensemble based Kalman filter and Massachusetts Institute of Technology general circulation model (MITgcm) ice-ocean coupled model, an advanced sea ice data assimilation and prediction system has been developed, and skillful sea ice predictions in the synoptic scale were obtained by assimilating Special Sensor Microwave Imager Sounder (SSMIS) sea ice concentration and SMOS/CryoSat-2 ice thickness (e.g., Yang et al., 2014; Yang et al., 2015a; Yang et al., 2015b; Yang et al., 2016a; Yang et al., 2016b; Mu et al., 2018a; Mu et al., 2018b). However, it is not clear whether this system can be extended to the operational seasonal prediction.

Towards a skillful operational Arctic sea ice seasonal outlook, in this study, we construct an ensemble based sea ice assimilation and prediction system for summer Arctic sea ice prediction. To better capture the large uncertainties in late summer, we have conducted a set of ensemble predictions of Arctic sea ice in summer 2016 using a coupled ice-ocean model. The summer of 2016 is chosen because that year had a record low maximum extent in March, a record low monthly extent in June, and the second lowest monthly extent in September (4.14 million square kilometers; http://nsidc.org/arcticseaicenews/2016/09/) since the satellite era. The 4-month sea ice concentration and thickness predictions which started from May 25 of 2016 are evaluated with satellite, reanalysis and *in-situ* observations. A detailed description of the prediction system is presented in Section 2, followed by experiment design in Section 3. The prediction evaluation and results are shown in Section 4. The sensitivity of the prediction system is shown in Section 5, and finally the discussion and conclusions are provided in Section 6.

2. Ensemble Based Sea Ice Seasonal Prediction System

The ensemble based Sea Ice Seasonal Prediction System (SISPS) uses the MITgcm sea ice-ocean model (Marshall et al., 1997, Losch et al., 2010). This model includes state-of-the-art sea ice dynamics based on Zhang and Hibler (1997) and simple zero-layer thermodynamics (Losch et al., 2010). An Arctic regional configuration with a horizontal resolution of about 18 km (Losch et al., 2010; Nguyen et al., 2011) is applied. The vertical resolution is higher in the upper ocean, with 28 vertical levels in the top 1000 m and additional 22 layers below 1000 m. Bathymetry is derived from the US National Geophysical Data Center (NGDC) 2 min global relief dataset (ETOPO2: Smith and Sandwell, 1997). The monthly mean river runoff is based on the Arctic Runoff Data Base (ARDB). Climatological oceanic fields from the Estimating the Circulation and Climate of the Ocean, Phase II (ECCO2) are prescribed for the open boundary conditions.

To provide the “best possible” initial ice-ocean conditions for SISPS prediction, a retrospective simulation (CMST; Mu et al., 2018b) that assimilates satellite sea ice concentration and ice thickness was carried out. The CMST simulation is available during the SMOS and CryoSat-2 period from October 2010, and has been evaluated to be a good estimate on both winter and summer Arctic sea ice thickness (Mu et al., 2018b). As in Yang et al. (2015a, 2016) and Mu et al.(2018a), this simulation was also driven by the United Kingdom Met Office (UKMO) ensemble atmospheric forcing with 23 perturbed members from 1 January 2010 to 15 July 2014, and 11 perturbed members after 6 November 2014 while assimilating near-real-time SSMIS sea ice concentration, SMOS and CryoSat-2 sea ice thickness data. The SSMIS sea ice concentration is available all year round, but the SMOS/CryoSat-2 ice thickness is only available for the cold season from October to the next April. It should be noted that there is no near-real-time SMOS and CryoSat-2 ice thickness data available on May 26, 2016, the starting date of this seasonal prediction. However, the sea ice thickness assimilated in the cold season can provide a good initial state for the melt season when thickness data are not available, and the summer ice thickness can be corrected via the positive cross-correlations between ice concentration and thickness (Yang et al., 2015a; Mu et al., 2018b).

The atmospheric forcing fields for the seasonal outlook are obtained from the CFSv2. The daily CFSv2 prediction ranges from hours to months (Saha et al., 2014). The forecast runs go out to 9 months every day, and these data are used for seasonal prediction in this study. The CFSv2 provide 6-hourly atmospheric forecasting fields in real time. These fields are ideal for forcing ice-ocean models on daily to seasonal time scales. To match our ensemble data assimilation configuration with the CMST simulation (11 members in 2016), here we use 11 CFSv2 forecast ensemble members, which include 1 forecast on the prediction day (25 May 2016) and 10 forecasts from the previous days (4 forecasts from 24 May, 4 forecasts from 23 May, 2 forecasts from 22 May of 2016). A 48h-lagged forecast is one with valid time 48h in advance of the beginning of the seasonal forecast period, so 0h-lagged in Table 1 indicates the forecast that starts on 00:00 May 25 2016. All these predictions range from 00:00 25 May to 00:00 1 October of 2016. After the initialization, 11 ensemble sea ice-ocean forecasts are conducted using atmospheric forecasts from 11 CFSv2 ensemble runs, e.g., each of these 11 individual ensemble members is associated with a unique set of forcing fields and sea ice-ocean initial states from 25 May 2016 to 30 September 2016. During the seasonal prediction, SISPS uses these initialization fields from the CMST simulation, and runs forward without assimilating any satellite ice concentration and thickness data.

3. Validation and Sensitivity Experiment Design

As a reference, the operational seasonal CFSv2 sea ice prediction started from 00:00 25 May in 2016 is also evaluated and compared with our results. The sea ice model used in CFSv2 is based on the Geophysical Fluid Dynamics Laboratory (GFDL) Sea Ice Simulator. Different from SISPS, it has three layers for thermodynamics, and uses the elastic–viscous–plastic technique (EVP; Hunke and Dukowicz, 1997) for sea ice dynamics. The initial condition for sea ice in the CFSv2 hindcast is from the NCEP Climate Forecast System Reanalysis (CFSR) that assimilates the near-real-time SSMIS sea ice concentration from the National Snow and Ice Data Center (NSIDC; Cavalieri et al., 1996; http://nsidc.org/data/nsidc-0081) with a simple nudging scheme. Note that although CFSR has a modeled ice thickness, there is no sea ice thickness assimilation. For details, the readers are referred to Saha et al. (2010).

The sea ice concentration from NSIDC, the PIOMAS ice thickness reanalysis, the CMST ice thickness and the in-situ ice thickness from the Beaufort Gyre Exploration Project (BGEP; http://www.whoi.edu/beaufortgyre) are used for evaluation. The PIOMAS system consists of the Parallel Ocean Program (POP) and a 12-category thickness and enthalpy distribution sea ice model on a generalized curvilinear coordinate. This system is forced by NCEP/NCAR reanalysis. Daily sea ice concentration from NSIDC and sea surface temperature from the NCEP/NCAR reanalysis are assimilated with nudging and optimal interpolation (Zhang and Rothrock, 2003; Schweiger et al., 2011). The BGEP deploys upward looking sonar (ULS) moorings at three locations BGEP A, BGEP B and BGEP D every year since 2003, and the ULS can measure the ice draft with an error of about 0.1m (Melling et al., 1995). Following Nguyen et al. (2011), drafts are converted to thicknesses by simply multiplying with a factor of 1.1. The locations of ULS sites were listed in Figure 1 of Yang et al. (2015).

To study the sensitivity of the SISPS prediction to different sea ice initializations and atmospheric forcing, four more experiments are conducted in addition to the control run (SISPS as described in Section 2) as shown in

Table 1. The deterministic prediction experiment DP-CMST is driven by 0h-lagged CFSv2 forcing, which is right on the prediction start date and is expected to be the most realistic because of the better initial state after initialization in the CFSv2. The sea ice states in DP-CMST are initialized by the CMST ensemble mean. The experiment ENS-PIOMAS is configured as SISPS, but uses PIOMAS thickness to initialize the model thickness. The experiment DP-PIOMAS, however, is the deterministic prediction for ENS-PIOMAS. Sea ice thickness from the CFSv2 is also used to initialize the model thickness in an experiment named DP-CFS. The differences between DP-CFS and CFSv2 are that DP-CFS uses a different model with different initial sea ice concentration.

Table 1 Summary of the experiment configuration.*

	Sea ice initial condition	Atmospheric forcing	Data assimilation over the prediction period
SISPS	CMST SIC / CMST SIT	Time-lagged CFSv2 ensemble forcing	No
DP-CMST	CMST SIC / CMST SIT	0h-lagged CFSv2 forcing	No
ENS-PIOMAS	CMST SIC / PIOMAS SIT	Time-lagged CFSv2 ensemble forcing	No
DP-PIOMAS	CMST SIC / PIOMAS SIT	0h-lagged CFSv2 forcing	No
DP-CFS	CMST SIC / CFSv2 SIT	0h-lagged CFSv2 forcing	No

*SIC = Sea ice concentration, SIT = Sea ice thickness

4. SISPS Prediction Results

4.1 Sea ice extent and concentration

The sea ice extent is defined as the total area of the grids with ice concentration larger than 15%. The prediction is good for the date of the summer minimum around September 10 (Figure 1) from CFSv2 and SISPS. The SISPS summer extent minimum is 4.26 million km^2, which is slightly larger than the NSIDC observation (4.14 million km^2). However, a large overestimation of 3.83 million km^2 (a relative overestimation of 92.3%) is observed in the CFSv2 prediction. It should also be noted that SISPS significantly underestimates the ice extent in July. The underestimation is not clear at this moment. It may be related to the stormy conditions in July and August of 2016 (http://nsidc.org/arcticseaicenews/2016/09/), which, however, is beyond the capability for CFSv2 to predict realistic synoptic weather 2 months ahead.

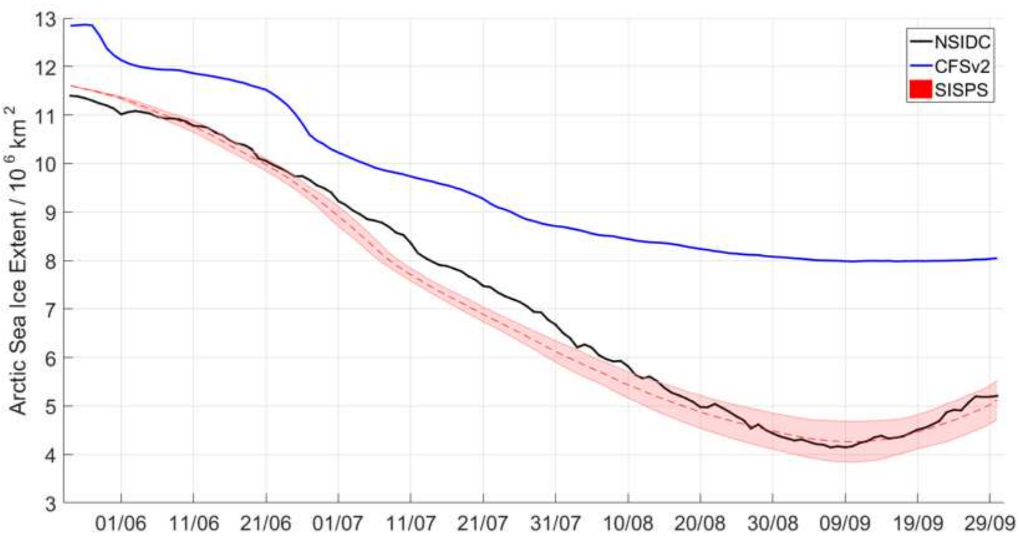

Figure 1 Evolution of Arctic sea ice extent from 25 May to 30 September in 2016. The NSIDC observations and CFSv2 forecasts are shown as black and blue solid lines, respectively. The ensemble mean and the spread of SISPS forecasts are shown as red dashed lines and red shades. Date format is dd/mm.

Figure 2 shows the sea ice extent prediction in six different Arctic regions, as defined on Figure 1 in Cavalieri and Parkinson (2012). The CFSv2 overestimates sea ice extent in most of the Arctic regions, in particular there is an overestimation of 3.5 million km^2, 0.6 million km^2 and 0.3 million km^2 in the Central Arctic Ocean, the Kara and Barents Seas and the Canadian Archipelago on September 10 of 2016 (the Arctic summer minimum), respectively. Thesecan also be seen in Figure 3, in which it shows the sea ice concentration averaged over the period from 30 August to 19 September, 2016. In contrast, the ensemble mean of SISPS agrees well with the NSIDC observations in most of the regions, particularly in the central Arctic Ocean (Figure 2) and in September. However, the predicted ice extent in Kara and Barents Seas are highly overestimated in June and July, and the maximum overestimation reaches 0.5 million km^2. Sea ice in Kara and Barents Seas was well below average in winter and spring of 2016, and the surface conditions were unusually warm, therefore sea ice extent in June and July of 2016 were significantly lower than the normal level (http://nsidc.org/arcticseaicenews/2016/07/). In this situation, SISPS fails to capture the abnormal sea ice changes due to imperfect atmospheric conditions from the prediction.

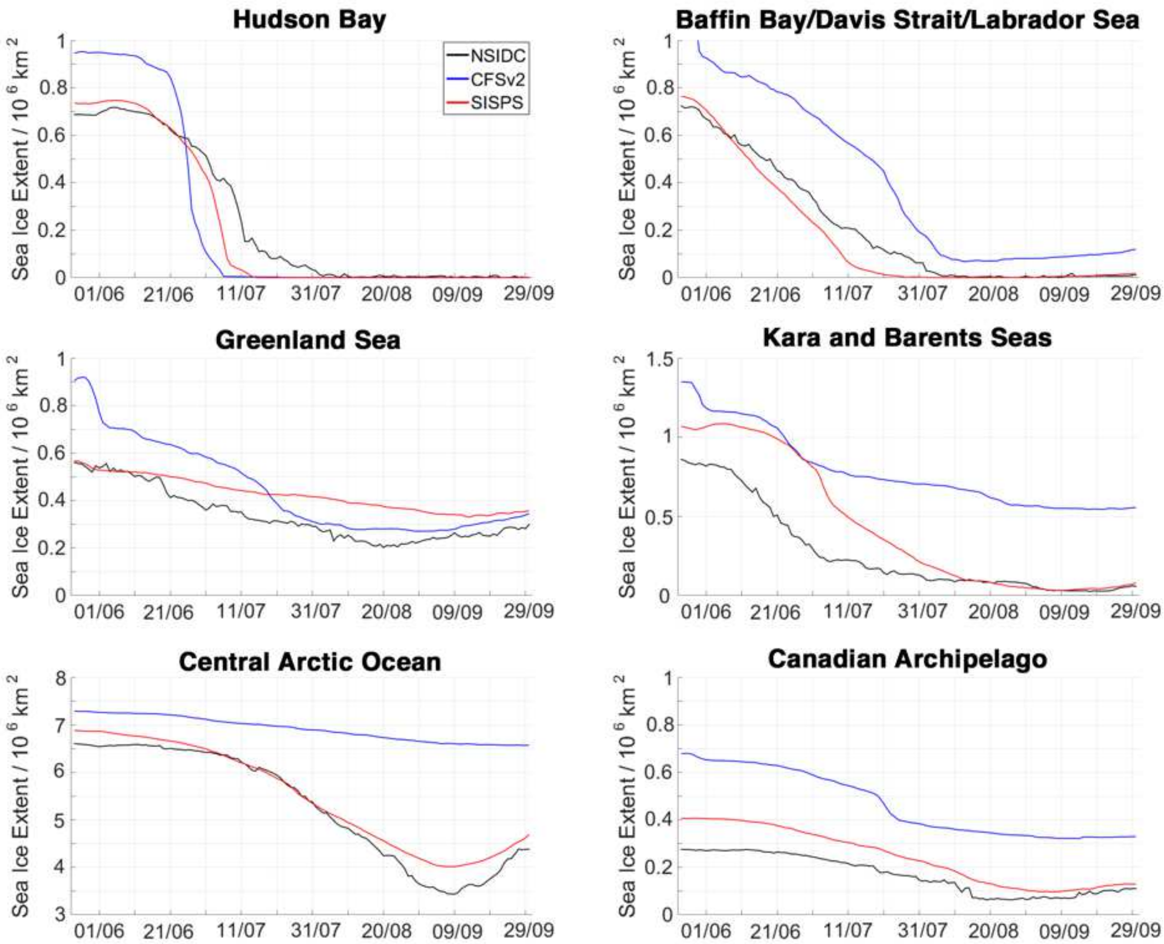

Figure 2 Evolutions of sea ice extent in different Arctic regions from 25 May to 30 September in 2016. The NSIDC observations, CFSv2 and ensemble mean of SISPS forecasts are shown as black, blue and red solid lines, respectively.

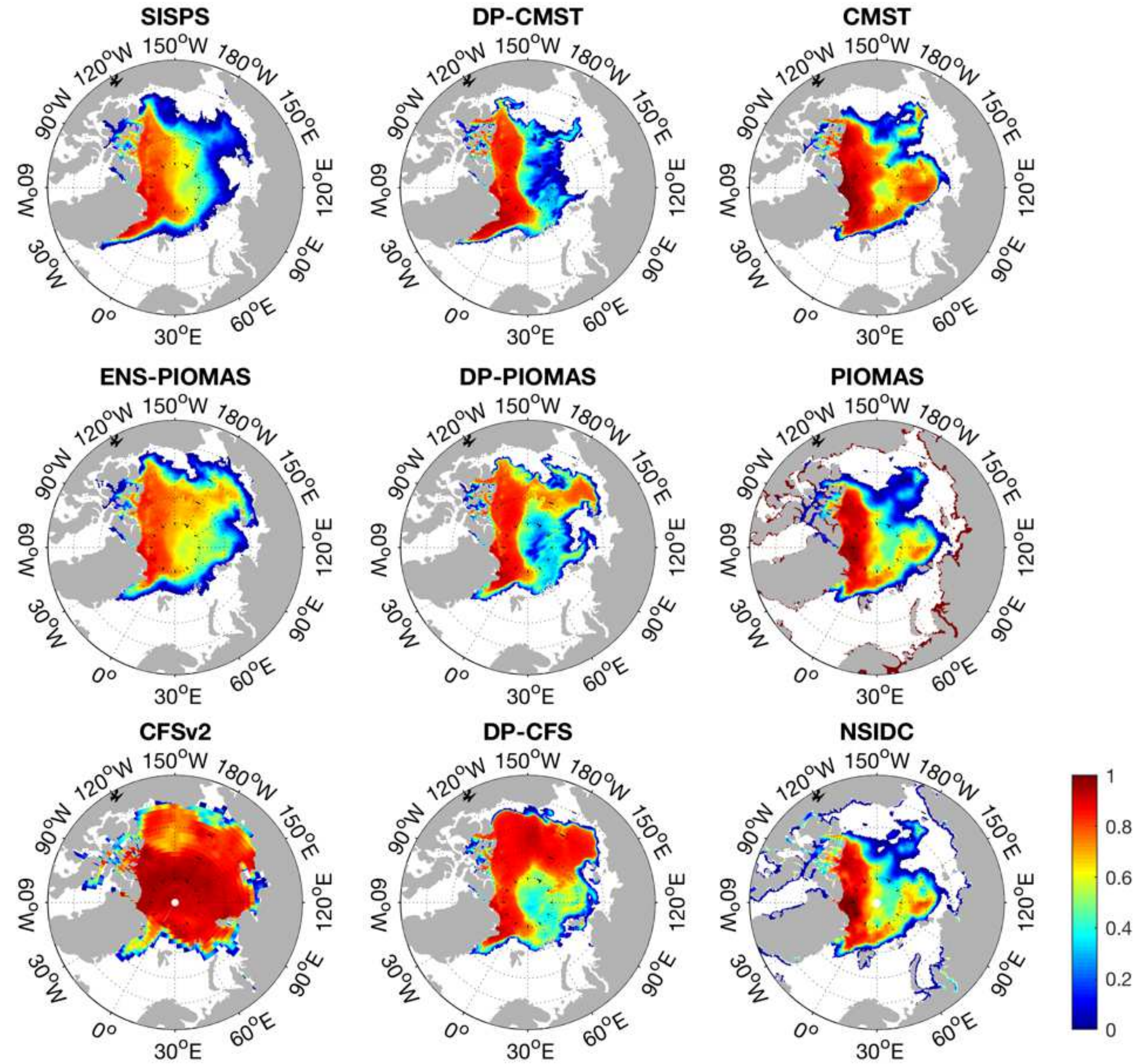

Figure 3 Sea ice concentration averaged over the period from 30 August to 19 September, 2016. Note that results from SISPS, CMST and ENS-PIOMAS are ensemble means. Both CMST and PIOMAS assimilate sea ice concentration over this period and, moreover, sea surface temperature is also assimilated in PIOMAS. DP indicates experiments with single deterministic forcing, and ENS indicates the experiment with ensemble CFSv2 forcing.

The temporal evolution of root-mean-square error (RMSE) differences between the predictions with the NSIDC sea ice concentration observations are shown in Figure 4. Following Lisæter et al. (2003) and Yang et al. (2015), the RMSE is only calculated at grid points where either the forecasts or the observations have ice concentration larger than 0.05. The RMSE of the ensemble mean SISPS prediction (the blue solid line) is 0.34 in the beginning of the prediction, and is basically stable within a range between 0.28 and 0.34 over the 4-month prediction period. The CFSv2 has even lower RMSE values than the SISPS ensemble mean in the first 25 days (before June 19; the blue dashed line), which shows some prediction skill on the sea ice concentration during this period. This is expected because the CFSv2 system operationally nudges the NSIDC sea ice observations which are also used in this validation. However, in contrast to SISPS, the RMSE of CFSv2 prediction keeps increasing and reaches a maximum of 0.57 on 8 September of 2016, which also demonstrates a large error in the seasonal summer sea ice prediction in the operational CFSv2 system.

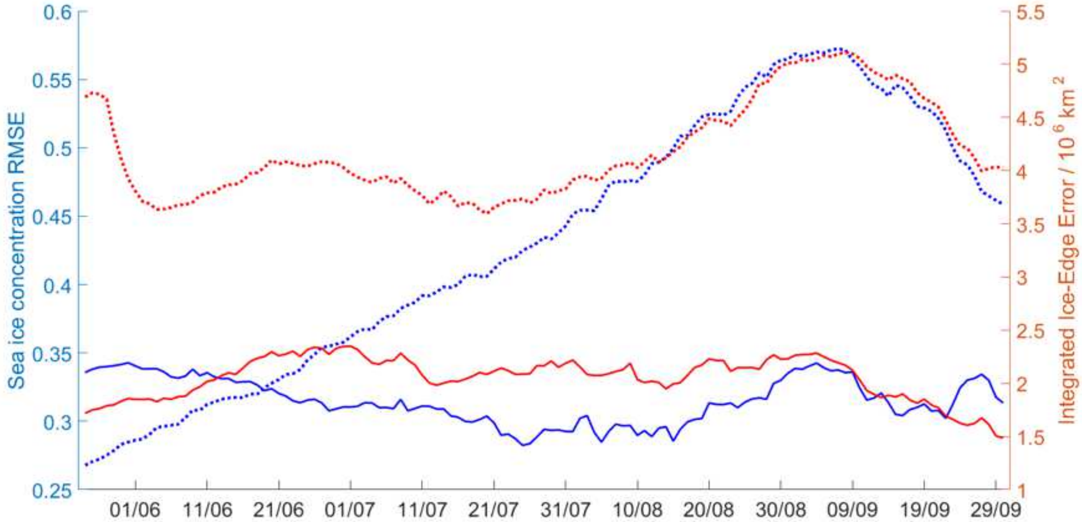

Figure 4 Evolution of RMSE differences (blue) and the integrated ice-edge error (IIEE; red) with respect to the NSIDC ice concentration data from 25 May to 30 September in 2016, the SISPS ensemble mean and the CFSv2 predicted sea ice concentration are shown as solid and dashed lines, respectively.

Here the integrated ice-edge error (IIEE; Goessling et al., 2016) is used as an additional metric. It shows the total area of grid cells, where there is a mismatch between the model and satellite data in the presence of sea ice. The IIEE of SISPS (the red solid line in Figure 4) is always significantly lower than that of CFSv2 (the red dashed line) during the 4-month prediction period. The mean IIEE during this period for SISPS is 2.05 million km^2, while that for CFSv2 is 4.19 million km^2. The difference is substantial with about 2.14 million km^2 that is more than half of the CFSv2 IIEE values.

The predicted sea ice concentration varies considerably among the 11 ensemble members, in particular in September (Figure 5). The ensemble standard deviation of sea ice concentration is very small in the beginning of the prediction, but it keeps increasing with the prediction time, and finally reaches a maximum in late September. The predicted deviation (prediction uncertainties) is relatively small in the central Arctic where the sea ice concentration is close to 100%, and large in the marginal ice zones where sea ice changes dramatically (Figure 5). This spatial distribution and ensemble spread fit well to the standard deviation of sea ice concentration calculated based on SSMIS observations over the period from 2006 to 2016 (also 11 members, figure not shown). It demonstrates that the ensemble spread of SSMIS is able to mimic the interannual variability in reality.

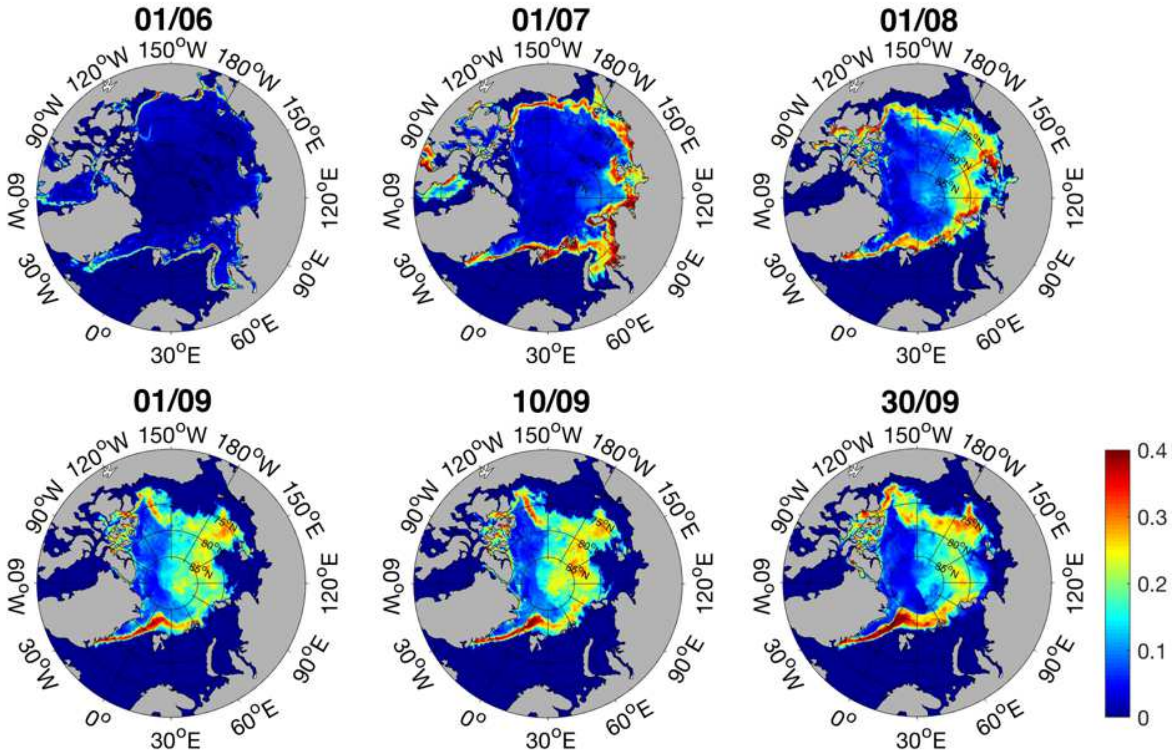

Figure 5 The ensemble standard deviation (SD) of sea ice concentration for SISPS on 1 June, 1 July, 1 August, 1 September, 10 September, and 30 September, 2016.

4.2 Sea ice thickness

SISPS sea ice thickness prediction averaged over the period from 30 August to 19 September 2016 is shown in Figure 6. The SISPS prediction agrees well with CMST and PIOMAS thickness (Figure 6). Sea ice thickness in the East Siberian and Laptev Seas is underestimated by SISPS, while appears promising over thick ice (> 1.0 m) area. SISPS also predicts more ice along east coast of Greenland. Apparently, CFSv2 highly overestimates sea ice thickness in the central Beaufort Sea and the Arctic marginal seas (Figure 6). The spatial distribution of CFSv2 thickness seems not reasonable comparing to the well-recognized PIOMAS reanalysis. Similar to the ice concentration prediction, the SISPS shows better prediction skill over the CFSv2 prediction.

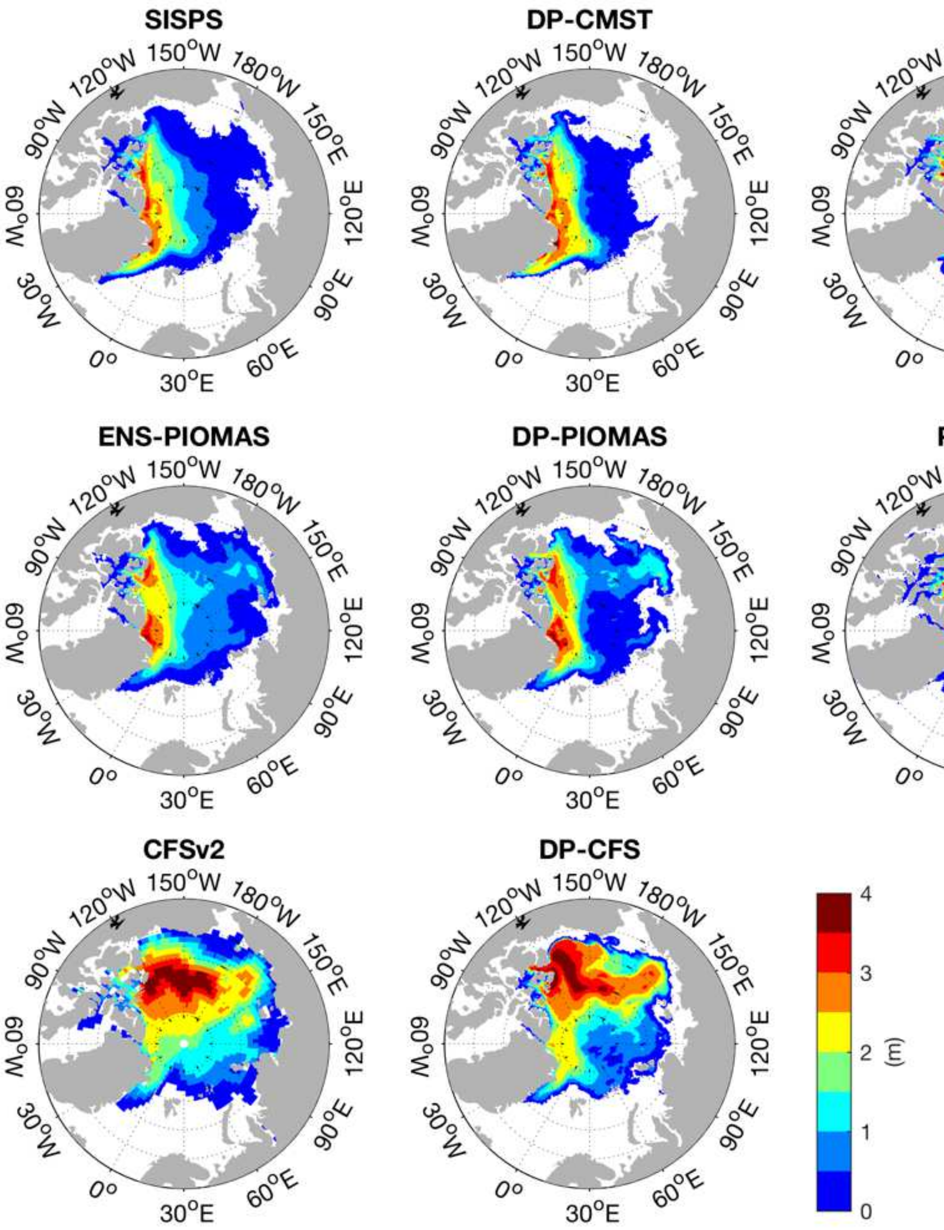

Figure 6 Sea ice thicknesses averaged over the period from 30 August to 19 September, 2016. Note that results from SISPS, CMST and ENS-PIOMAS are ensemble means. Both CMST and PIOMAS assimilate sea ice concentration over this period and, moreover, sea surface temperature is also assimilated in PIOMAS. DP indicates experiments with single deterministic forcing, and ENS indicates the experiment with ensemble CFSv2 forcing.

The time series of sea ice thickness predictions are compared to *in-situ* ULS-observations BGEP_2015A (Figure 7a), BGEP_2015B (Figure 7b) and BGEP_2015D (Figure 7c). At the site BGEP_2015A, the ice thickness RMSE of CFSv2, SISPS, CMST and PIOMAS with respect to the observations are 2.49 m, 0.40 m, 0.39 m and 0.39 m, respectively; at the site BGEP_2015B, they are 3.17 m, 0.31m, 0.33 m and 0.27 m, respectively; at the site BGEP_2015D, they are 2.34 m, 0.53 m, 0.50 m and 0.51 m, respectively. It is plausible that the 4-month sea ice thickness prediction of SISPS agrees well with the *in-situ* observations, and is comparable with the PIOMAS and CMST ice thickness estimates. CFSv2 overestimates sea ice thickness in the Beaufort Sea by as much as up to 2 m as also shown in Figure 6.

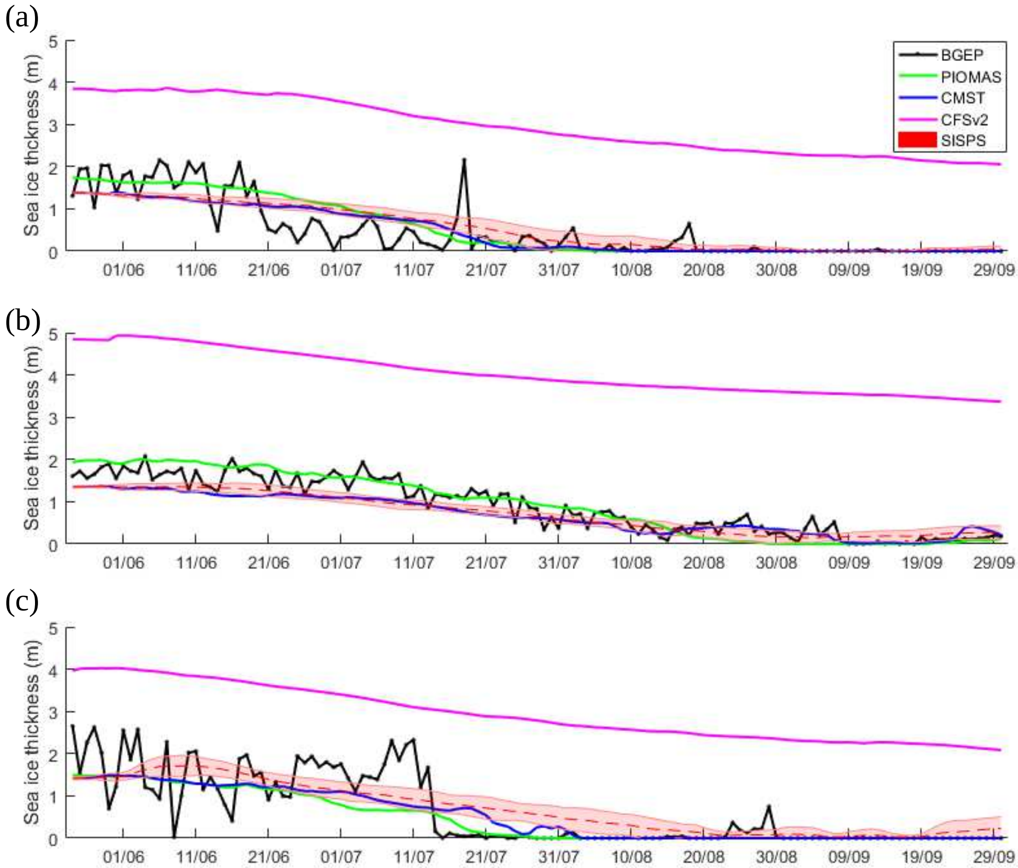

Figure 7 Evolution of mean sea ice thickness (m) at (a) BGEP_2015A, (b) BGEP_2015B and (c) BGEP_2015D Beaufort Sea from 25 May to 30 September 2016. The BGEP, PIOMAS, CMST, and CFSv2 thickness are shown as black, green, blue, magenta and red solid lines, respectively. The ensemble mean and the spread of SISPS forecasts are shown as red dashed lines and red shades.

Similar to the ice concentration prediction, the ensemble spread of the predicted sea ice thickness also varies considerably among the 11 ensemble members with time evolution (Figure 8), but shows differences on spatial distribution. In early summer (e.g., 1 July) the ensemble deviation of sea ice thickness is small (< 0.1m) in the central Arctic Ocean and large (> 0.4 m) in the marginal sea ice zone (Figure 8), which is consistent with the sea ice concentration (Figure 5), Over the melting period, the deviation becomes larger (> 0.4 m) in the central Arctic.

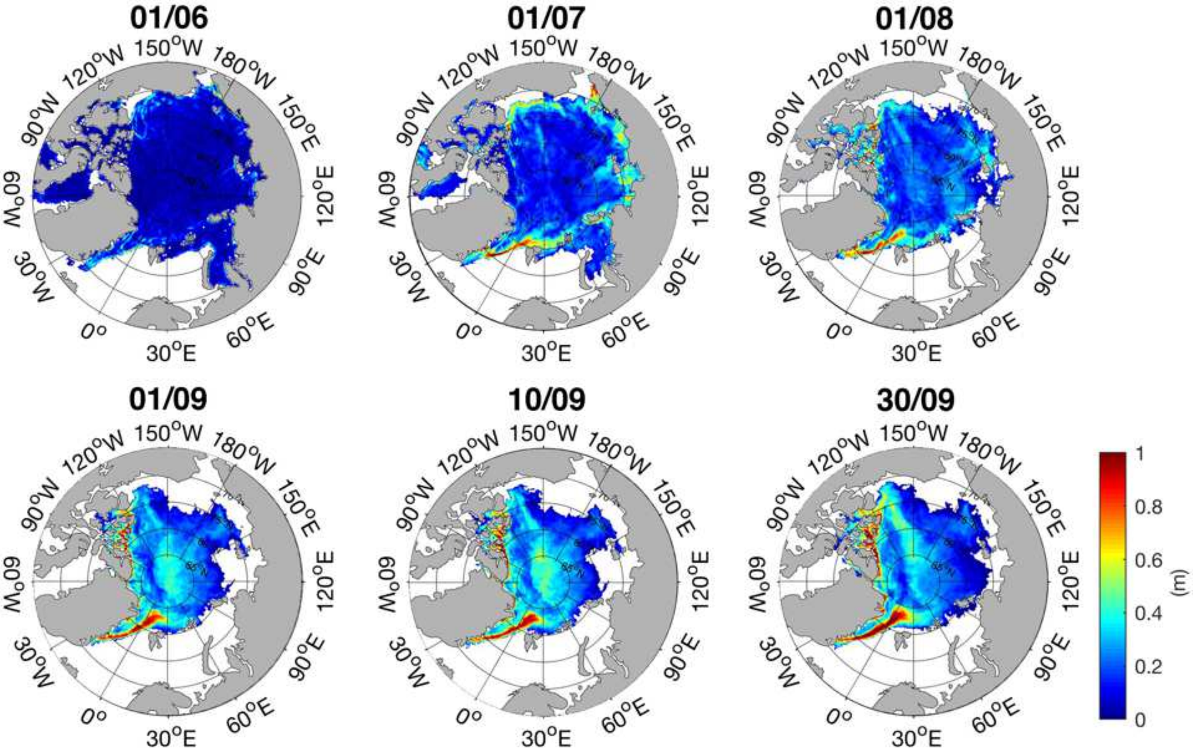

Figure 8 The ensemble standard deviation (SD) of sea ice thickness for SISPS on 1 June, 1 July, 1 August, 1 September, 10 September, and 30 September in 2016.

5. Sensitivity of SISPS in seasonal sea ice prediction

The uncertainty of sea ice prediction using an ice-ocean coupled model may be attributed to shortcomings in model physics and improper atmospheric forcing. The initial condition plays an important role on long-term prediction in the presence of such uncertainties. SISPS sea ice prediction benefits from both the initial states from the CMST ensemble and the time-lagged ensemble forcing from the CFSv2.

As shown in Figures 3 and 6, with reasonable sea ice thickness initialization, SISPS, DP-CMST, ENS-PIOMAS and DP-PIOMAS all predicted better September sea ice concentration and thickness than the CFSv2 and DP-CFS did. However, even with the same sea ice concentration initialization as DP-CMST and DP-PIOMAS, sea ice concentration from DP-CFS is far away from reality, so is the sea ice thickness. This indicates that a realistic sea ice thickness initialization is crucial for seasonal prediction, as also reported by other studies (Blockley et al., 2018; Collow et al., 2015; Xie et al., 2018). It is worth noting that although CMST and PIOMAS sea ice thickness can be both considered as good estimates in the Arctic (CMST versus PIOMAS in Figure 6), the initialization of using CMST or PIOMAS thickness can still lead great differences in predicting September sea ice thickness (Figures 3 and 6; DP-CMST versus DP-PIOMAS). Sea ice thickness and concentration are underestimated north of Laptev Sea. In DP-CMST sea ice concentration and thickness are also underestimated north of the East Siberian Sea, but they are overestimated in DP-PIOMAS there.

The initial sea ice extent also plays a substantial role on September sea ice extent prediction, but not on ice concentration and thickness prediction in our study. In DP-CFS the initial sea ice concentration from CMST is used, which is closer to the NSIDC observation as shown in Figure 1, therefore the initial sea ice extent for DP-CFS is considered reasonable. The September sea ice extent prediction from DP-CFS outperforms CFSv2 (Figures 3 and 6) over the Arctic marginal seas. Chevallier et al. (2013) also confirmed that the anomaly of spring sea ice cover preconditions the September SIE anomaly. However, a better sea ice concentration initial condition alone does not give rise to a promising September sea ice concentration (DP-CFS in Figure 3) and sea ice thickness (DP-CFS in Figure 6).

The ensemble forcing, another important influencing factor for sea ice prediction, has improved the prediction for both ice concentration and ice thickness (SISPS and ENS-PIOMAS in Figures 3 and 6). The ensemble forcing not only reduces uncertainties in the atmospheric forcing but also corrects ice-ocean model uncertainties due to model deficiencies such as different sea ice parameters in different models (e.g., Massonnet et al., 2014). As shown in Figure 9, the 0h-lagged CFSv2 atmospheric forecast (red line) does not always have the lowest root-mean-square (RMS) differences with respect to ERA-Interim atmospheric reanalysis according to the calculation of downward longwave radiation, downward shortwave radiation and 2 m temperature. The 66h-lagged forecast even performs better, such as the 2 m temperature forecast in June and July (Figure 9c) and the downward shortwave radiation forecast in June (Figure 9b). The ensemble forcing provides atmospheric trajectories with also wide probability for the prediction. In SISPS thicker and more ice is predicted over the area near North Pole towards the Eurasian continent, but it is underestimated in DP-CMST over the same area. ENS-PIOMAS also reduces the biases of DP-PIOMAS over this area and north of East Siberian Sea.

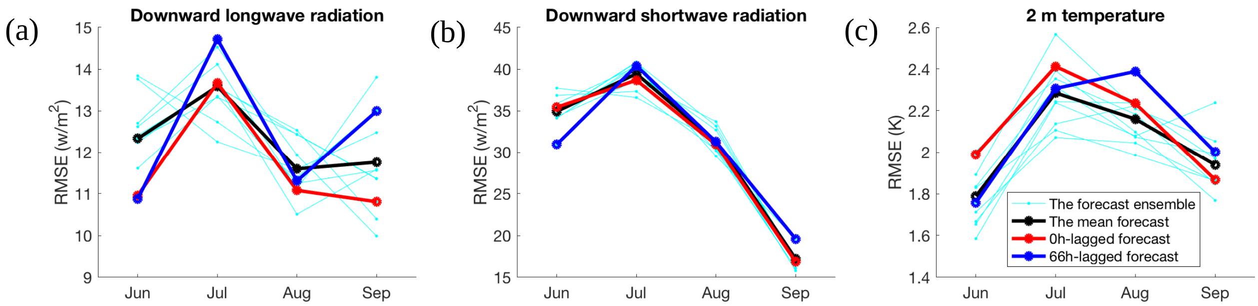

Figure 9 RMS differences of monthly mean downward longwave radiation (a), downward shortwave radiation (b), and 2 m temperature (c) in the ensemble forcing with respect to ERA-Interim atmospheric reanalysis. Note that the 0h-lagged forecast was initialized in CFSv2 right on the prediction start (00:00:00 25 May 2016), while the 66h-lagged forecast was initialized 66 hours before the prediction start.

6. Discussion and conclusions

In an effort to operationally predict the summer sea ice on seasonal time scale, an ensemble based Seasonal Sea Ice Prediction System (SISPS) is configured and a 4-month hindcast experiment is carried out to predict the summer sea ice in 2016. The initialization for the experiment uses the restart files from the CMST system that assimilates near-real-time satellite sea ice observations, specifically the sea ice concentration from SSMI and/or SSM/IS channels and the sea ice thickness from SMOS and CryoSat-2. Zhang et al. (2008) implemented a 1-year sea ice prediction system using unchanging initial sea ice-ocean fields but with an ensemble of different atmospheric forcing. In this study, we extend the outlook with an ensemble of both different sea ice-ocean initialized fields and different atmospheric forcing fields. The relatively large ensemble standard deviations in September in SISPS are comparable to the natural variability calculated from 2006 to 2016. Evaluations with observations demonstrate that prediction results from SISPS are very promising. The results from the additional sensitivity experiments indicate that the proper sea ice initial conditions and ensemble atmospheric forcing in SISPS contribute to a better prediction.

As illustrated in Zhang et al. (2008), one difficulty in the ensemble predictions is the lack of operational prediction forcing since the ice-ocean model does not include an atmospheric component. Zhang et al. (2008) used the NCEP/NCAR reanalysis forcing fields from 2000 to 2007 for various individual ensemble predictions to drive PIOMAS sea ice-ocean model, while Zhang and Schweiger used the daily four atmospheric seasonal forecasts from the CFSv2 in their seasonal sea ice outlook for 2017. As a further extension, in this study we increase the ensemble members to 11 to match our ensemble initializations, and to better reflect the prediction uncertainties, by using a time-lagged ensemble of 11 operational atmospheric forcing which from the CFSv2 system.

The second difficulty described in Zhang et al. (2008) is the lack of reasonable initial ensemble sea ice-ocean state. Our initial sea ice-ocean fields are from the CMST simulation, in which the near-real-time SSMIS sea ice concentration, SMOS and CryoSat-2 ice thickness are assimilated, and had been proven to be a good estimate on the year-round Arctic sea ice thickness (Mu et al., 2018b). The SISPS predicts a much better sea ice distribution than the CFSv2 does, although the operational atmospheric forcing fields from the CFSv2 are used to drive SISPS. This reflects the importance of assimilating satellite based sea ice concentration and thickness observations with an advanced data assimilation method, though there is no available sea ice thickness observations on the prediction starting date (May 25 of 2016). The multivariate data assimilation system helps correct the sea ice thickness by providing a good initial state for the upcoming melt season and updating the summer thickness with assimilation of sea ice concentration only, because there is a positive correlation between sea ice concentration and thickness in summer, which can be explained by sea ice thermodynamics that the thick ice can reduce the horizontal melting (Yang et al., 2015; Mu et al., 2018b). However, in CFSv2 it only assimilates sea ice concentration with a simple nudging scheme, ice thickness cannot be corrected during the assimilation, thus the overestimation of the Arctic sea ice thickness in CFSv2 remains unchanged. It is expected that the sea ice prediction can be largely corrected by reducing the initial sea ice thickness error if the CryoSat-2 and SMOS ice thickness are assimilated in CFSv2 (Chen et al., 2017). The systematic errors should be considered and treated carefully when using the CFSv2 for seasonal sea ice predictions.

Although this is only a case study towards developing an operational sea ice seasonal prediction system to predict summer sea ice conditions, this SISPS system has shown great potential for seasonal sea ice prediction. Nevertheless, more applications with this system for seasonal sea ice prediction can be applied in the future, the robustness of the system can be further tested.

Acknowledgments This is a contribution to the Year of Polar Prediction (YOPP), a flagship activity of the Polar Prediction Project (PPP), initiated by the World Weather Research Programme (WWRP) of the World Meteorological Organisation (WMO). We thank the University of Hamburg for providing SMOS sea ice thickness data and sea ice concentration data, the National Snow & Ice Data Center (NSIDC) for sea ice concentration data, the Alfred Wegener Institute (AWI) for the CryoSat-2 sea ice thickness data, the Woods Hole Oceanographic Institution for the sea ice draft data, the European Centre for Medium-Range Weather Forecasts and UKMO for the atmospheric forcing data. This study is supported by National Key R&D Program of China (2018YFA0605901), the Opening fund of State Key Laboratory of Cryospheric Science (SKLCS-OP-2019-09), the Federal Ministry of Education and Research of Germany in the framework of SSIP (grant01LN1701A), and the National Natural Science Foundation of China (41776192, 41706224). JZ was supported by the US NSF grants PLR-1416920 and PLR-1603259.

References

Blanchard-Wrigglesworth, E., Armour, K. C., Bitz, C. M., DeWeaver, E., 2011. Persistence and inherent predictability of Arctic sea ice in a GCM ensemble and observations. J. Climate. 24(1), 231-250.

Blockley, E. W., Peterson, K. A., 2018. Improving Met Office seasonal predictions of Arctic sea ice using assimilation of CryoSat-2 thickness. Cryosphere. 12, 3419-3438, https://doi.org/10.5194/tc-12-3419-2018.

Chen, Z., Liu, J., Song, M., Yang, Q., Xu, S., 2017. Impacts of assimilating satellite sea ice concentration and thickness on Arctic sea ice prediction in the NCEP climate forecast system. J. Climate. doi: 10.1175/JCLI-D-17-0093.1.

Chevallier, M., Salas-Mélia, D., 2012. The role of sea ice thickness distribution in the Arctic sea ice potential predictability: A diagnostic approach with a coupled GCM. J. Climate. 25(8), 3025-3038.

Chevallier, M., Salas y Mélia, D., Voldoire, A., Déqué, M. and Garric, G., 2013. Seasonal forecasts of the pan-Arctic sea ice extent using a GCM-based seasonal prediction system. Journal of Climate, 26(16), pp.6092-6104.

Collow, T.W., Wang, W., Kumar, A. and Zhang, J., 2015. Improving Arctic sea ice prediction using PIOMAS initial sea ice thickness in a coupled ocean–atmosphere model. Monthly Weather Review, 143(11), pp.4618-4630.

Day, J. J., Hawkins, E., Tietsche, S., 2014. Will Arctic sea ice thickness initialization improve seasonal forecast skill? Geophys. Res. Lett. 41, 7566-7575, doi:10.1002/2014GL061694.

Goessling, H.F., Tietsche, S., Day, J. J., Hawkins, E., Jung, T. 2016. Predictability of the Arctic sea ice edge. Geophys. Res. Lett. 43: 1642–1650.

Hunke, E.C. and Dukowicz, J.K., 1997. An elastic–viscous–plastic model for sea ice dynamics. Journal of Physical Oceanography, 27(9), pp.1849-1867.

Jung, T., Gordon, D. N., Bauer, P., Bromwich, D. H., Chevallier, M., Day, J. J., Dawson, J., Doblas-Reyes, F., Fairall, C., Goessling, H. F., Holland, M., Inoue, J., Iversen, T., Klebe, S., Lemke P., Losch M,, Makshtas A., Mills, B., Nurmi, P., Perovich, D., Reid, P., Renfrew, I. A., Smith, G., Svensson, G., Tolstykh, M., Yang, Q. 2016. Advancing polar prediction capabilities on daily to seasonal time scales. Bull Amer Meteor Soc. doi: 10.1175/BAMS-D-14-00246.1.

Kauker, F., Kaminski, T., Ricker, R., Toudal-Pedersen, L., Dybkjaer, G., Melsheimer, C., Eastwood, S., Sumata, H., Karcher, M., Gerdes, R. 2015. Seasonal sea ice predictions for the Arctic based on assimilation of remotely sensed observations. Cryosphere Discuss. 9, 5521-5554, https://doi.org/10.5194/tcd-9-5521-2015.

Kimmritz, M., Counillon, F., Bitz, C. M., Massonnet, F., Bethke, I., Gao, Y. 2018. Optimising assimilation of sea ice concentration in an Earth system model with a multicategory sea ice model. Tellus. Series A, Dynamic meteorology and oceanography. 70:1435945.

Kwok, R., Cunningham, G. F., 2015. Variability of Arctic sea ice thickness and volume from CryoSat-2. Phil. Trans. R. Soc. A. 373(2045), 20140157.

Lisæter, K. A., Rosanova, J., Evensen, G. 2003. Assimilation of ice concentration in a coupled ice–ocean model using the Ensemble Kalman filter. Ocean Dyn. 53(4), 368-388.

Liu, J., Curry, J. A., Wang, H., Song, M., Horton, R. M., 2012. Impact of declining arctic sea ice on winter snowfall. Proc. Nat. Acad. Sci. USA, 109 (11), 4074-4079, doi:10.1073/pnas.1114910109.

Losch, M., Menemenlis, D., Campin, J. M., Heimbach, P., Hill, C., 2010. On the formulation of sea-ice models, Part 1: Effects of different solver implementations and parameterizations. Ocean Modell., 33(1), 129-144.

Marshall, J., Adcroft, A., Hill, C., Perelman, L., Heisey, C., 1997. A finite-volume, incompressible Navier Stokes model for studies of the ocean on parallel computers. J. Geophys. Res., 102 (C3), 5753-5766, doi:10.1029/96JC02775.

Massonnet, F., Goosse, H., Fichefet, T., Counillon, F. 2014. Calibration of sea ice dynamic parameters in an ocean‐sea ice model using an ensemble Kalman filter. J. Geophys. Res.-Oceans, 119(7), 4168-4184.

Massonnet, F., Fichefet, T., Goosse, H, 2015. Prospects for improved seasonal Arctic sea ice predictions from multivariate data assimilation. Ocean Modelling. 88, 16-25. Melling, H., Johnston, P. H., Riedel, D. A., 1995. Measurements of the underside topography of sea ice by moored subsea sonar. J. Atmos. Oceanic Technol. 12(3), 589–602.

Mu, L., Yang, Q., Losch, M., Losa, S. N., Ricker, R., Nerger, L., Liang, X., 2018a. Improving sea ice thickness estimates by assimilating Cryosat-2 and SMOS sea ice thickness data simultaneously. Quart. J. Roy. Meteor. 144 (711), 529-538.

Mu, L., Losch, M., Yang, Q., Ricker, R., Losa, S., Nerger, L., 2018b. Arctic-wide sea-ice thickness estimates from combining satellite remote sensing data and a dynamic ice-ocean model with data assimilation during the CryoSat-2. J. Geophys. Res.-Oceans. doi:10.1029/2018JC014316.

Nguyen, A. T., Menemenlis, D., Kwok, R., 2011. Arctic ice-ocean simulation with optimized model parameters: Approach and assessment. J. Geophys. Res.-Oceans. 116, C04025, doi:10.1029/2010JC006573.

Ricker, R., Hendricks, S., Kaleschke, L., Tian-Kunze, X., King, J., Haas, C., 2017. A weekly Arctic sea-ice thickness data record from merged CryoSat-2 and SMOS satellite data. Cryosphere. 11, 1607-1623, doi:10.5194/tc-11-1607-2017.

Saha S., and co-authors. The NCEP Climate Forecast System Reanalysis. Bulletin of the American Meteorological Society, 91(8):1015-1057, 2010. doi: 10.1175/2010BAMS3001.1.

Saha, S., Moorthi, S., Wu, X., Wang, J., Nadiga, S., Tripp, P., Behringer, D., Hou, Y., Chuang, H., Iredell, M., Ek, M., Meng, J., Yang, R., Mendez, M. P., Dool, H. van den, Zhang, Q., Wang, W., Chen, M., Becker, E., 2014. The NCEP climate forecast system version 2. J. Climate. 27(6), 2185-2208.

Schweiger, A., Lindsay, R., Zhang, J., Steele, M., Stern, H., Kwok, R., 2011. Uncertainty in modeled Arctic sea ice volume. J. Geophys. Res.-Oceans. 116 (9), doi:10.1029/2011JC007084.

Smith, W. H. F, Sandwell, D. T., 1997. Global sea floor topography from satellite altimetry and ship depth soundings. Science. 277(5334), 1956–1962, doi: 10.1126/science.277.5334.1956.

Smith, G. C., Roy, F., Reszka, M., Surcel Colan, D., He, Z., Deacu, D., et al., 2015. Sea ice forecast verification in the Canadian global ice ocean prediction system. Quart. J. Roy. Meteor. 142(695), 659–671. https://doi.org/10.1002/qj.2555.

Stroeve, J. C., Markus, T., Boisvert, L., Miller, J., Barrett, A., 2014. Changes in Arctic melt season and implications for sea ice loss. Geophys. Res. Lett. 41(4), 1216-1225.

Tian-Kunze, X., Kaleschke, L., Maaß, N., Mäkynen, M., Serra, N., Drusch, M., Krumpen, T., 2014. SMOS-derived thin sea ice thickness: Algorithm baseline, product specifications and initial verification. Cryosphere. 8, 997–1018, doi:10.5194/tc-8-997-2014.

Xie, J., Counillon, F. and Bertino, L., 2018. Impact of assimilating a merged sea-ice thickness from CryoSat-2 and SMOS in the Arctic reanalysis. The Cryosphere, 12(11), pp.3671-3691.

Yang, Q., Losa, S. N., Losch, M., Tian-Kunze, X., Nerger, L., Liu, J., Kaleschke, L., Zhang, Z., 2014. Assimilating SMOS sea ice thickness into a coupled ice-ocean model using a local SEIK filter, J. Geophys. Res.-Oceans. 119 (10), 6680-6692, doi:10.1002/2014JC009963.

Yang, Q., Losa, S. N., Losch, M., Jung, T., Nerger, L., 2015a. The role of atmospheric uncertainty in arctic summer sea ice data assimilation and prediction. Quart. J. Roy. Meteor. 141 (691), 2314-2323.

Yang, Q., Losa, S. N., Losch, M., Liu, J., Zhang, Z., Nerger, L., Yang, H., 2015b. Assimilating summer sea-ice concentration into a coupled ice-ocean model using a LSIK filter. Ann. Glaciol. 56 (69), 38-44.

Yang, Q., Losch, M., Losa, S. N., Jung, T., Nerger, L., Lavergne, T., 2016a. Brief communication: The challenge and benefit of using sea ice concentration satellite data products with uncertainty estimates in summer sea ice data assimilation. Cryosphere. 10 (2), 761-774, doi:10.5194/tc-10-761-2016.

Yang, Q., Losch, M., Loza, S., Jung, T., Nerger, L., 2016b. Taking into account atmospheric uncertainty improves sequential assimilation of SMOS sea ice thickness data in an ice-ocean model. J. Atmos. Oceanic Technol. 33, 397-407, doi:10.1175/JTECH-D-15-0176. 1.

Zampieri, L., Goessling, H. F., Jung, T., 2018. Bright Prospects for Arctic Sea Ice Prediction on Subseasonal Time Scales. Geophysical Research Letters. doi: 10.1029/2018GL079394.

Zhang, J., Hibler, W. D., 1997. On an efficient numerical method for modeling sea ice dynamics. J. Geophys. Res.-Oceans. 102(C4), 8691-8702.

Zhang, J., Rothrock, D. A., 2003. Modeling global sea ice with a thickness and enthalpy distribution model in generalized curvilinear coordinates. Mon. Weather Rev. 131 (5), 845-861, doi:10.1175/1520-0493(2003)131h0845:MGSIWAi2.0.CO;2.

Zhang, J., Lindsay, R., Steele, M., Schweiger, A., 2008. What drove the dramatic retreat of arctic sea ice during summer 2007?. Geophys. Res. Lett., 35(11), doi: 10.1029/2008GL034005.